

High-Repetition-Rate Real-Time Automatic Mode-Locked Fibre Laser Enabled by a Pre-Stretch Technique

Chao Luo^{ID}, Guoqing Pu^{ID}, Weisheng Hu^{ID}, *Member, IEEE*, and Lilin Yi^{ID}

Abstract—To apply the real-time automatic mode-locking technique to mode-locked lasers with high repetition rates, we propose a pre-stretch technique, where a slice of dispersion is used to stretch the output pulses thereby reducing the required sampling rate and the bandwidth of the acquisition system. To illustrate, we demonstrate a real-time automatic mode-locked fibre laser with a repetition rate of 48 MHz, where a real-time feedback circuit with a 400-MSa/s analog-to-digital converter is used as the hardware backend. Given a fixed acquisition system, the correlation between the repetition rate and the optimum amount of dispersion is well discussed through comparing the countable threshold range for mode-locking discrimination. Furthermore, a conclusion based on experiments is drawn that, to apply automatic mode-locking technique, the minimum acquisition bandwidth should be above twice of the fundamental repetition rate, and the minimum sampling rate follows the Nyquist's law, which is four times of the fundamental repetition rate.

Index Terms—High-repetition-rate mode-locked laser, pre-stretch technique, real-time automatic mode-locking.

I. INTRODUCTION

ULTRASHORT pulses have a wide range of applications in material processing [1], [2], frequency comb spectrum [3], biological imaging [4], [5], high-resolution atomic clocks [6], [7], astronomy [8] and precise measurements [9]. The nonlinear-polarization-evolution (NPE)-based mode-locked fibre laser (MLFL) is one of the important means of generating ultrashort pulses for its simple structure. However, the stability of the NPE-based MLFL is substantially challenged by the uncontrollable surroundings, resulting in the problem of hard to lock and frequent detachments for the laser. To enhance the stability of the NPE-based MLFL, the electrical-control-based automatic mode-locked lasers (AMLs) [10]–[20] have promptly emerged in recent years. The earliest AML is realized by traversing the parametric space using the electrical-optic components inside the cavity, such as the polarization Poincare sphere [10], [11]. Thereafter, various optimization algorithms are introduced to accelerate the process of parameter space searching for various

pulsation states [12], [13]. Due to the rapid development of computer science, machine learning and deep learning have been applied to AMLs as well [14], [15].

Nevertheless, most of the current AMLs have a relatively low repetition rate (i.e., below 20 MHz) and are achieved by the off-line feedback using large equipment, such as the oscilloscope and the optical spectrometer [16]. Previously, we realized a real-time AML based on a real-time feedback scheme including field-programmable gate array (FPGA) and a 400-MSa/s analog-to-digital converter (ADC) [17] whereas the repetition rate was only ~ 7.2 MHz, which was limited by the sampling rate of the ADC. On the other hand, an AML with a repetition rate of 59.5 MHz AML was demonstrated, while the experiment was conducted in an off-line feedback scheme using an optical spectrometer [18]. The MLFL with a higher repetition rate represents a higher fresh rate, which is preferred in most metric applications [21], [22]. Therefore, the real-time AML with a high repetition rate is in urgent need.

However, the high-repetition-rate real-time AML demands a high-speed acquisition device (i.e., up to GSa/s level) for information acquisition serving as the feedback input, which impedes the design of the real-time feedback hardware and increases the cost with no doubt. In this letter, we propose a pre-stretch technique using dispersion, which allows achieving the high-repetition-rate real-time AML using the low-sampling-rate and small-bandwidth acquisition system. Concretely, a real-time AML with a repetition rate of 48 MHz is realized in virtue of the pre-stretch technique. Further, the correlations among key parameters including the dispersion amount for pre-stretch, the detection bandwidth and the sampling rate of the acquisition device are illuminated, which ensures the proposed pre-stretch technique can be extended to use in AMLs with even-higher repetition rates.

II. PRINCIPLES AND RESULTS

The temporal-pulse-counting-based discrimination of the mode-locking states proves to be valid in our previous study [17], where the mode-locking state is discriminated by comparing the actual pulse count to the ideal pulse count derived from the repetition rate of the laser, the sampling rate of the ADC, and the number of sampling points. A high repetition rate represents a shorter period in the time domain. Given a fixed sampling rate, the number of sampling points in the pulse region is substantially reduced, hindering the discrimination via pulse counting. One solution to the pulse-counting-based discrimination problem is to broaden the pulses in order

Manuscript received 18 April 2022; revised 17 June 2022; accepted 21 June 2022. Date of publication 29 June 2022; date of current version 14 July 2022. This work was supported by the National Natural Science Foundation of China under Grant 62025503. (Corresponding author: Lilin Yi.)

The authors are with the State Key Laboratory of Advanced Optical Communication Systems and Networks, Shanghai Jiao Tong University, Shanghai 200240, China (e-mail: lilinyi@sjtu.edu.cn).

Color versions of one or more figures in this letter are available at <https://doi.org/10.1109/LPT.2022.3185989>.

Digital Object Identifier 10.1109/LPT.2022.3185989

1041-1135 © 2022 IEEE. Personal use is permitted, but republication/redistribution requires IEEE permission. See <https://www.ieee.org/publications/rights/index.html> for more information.

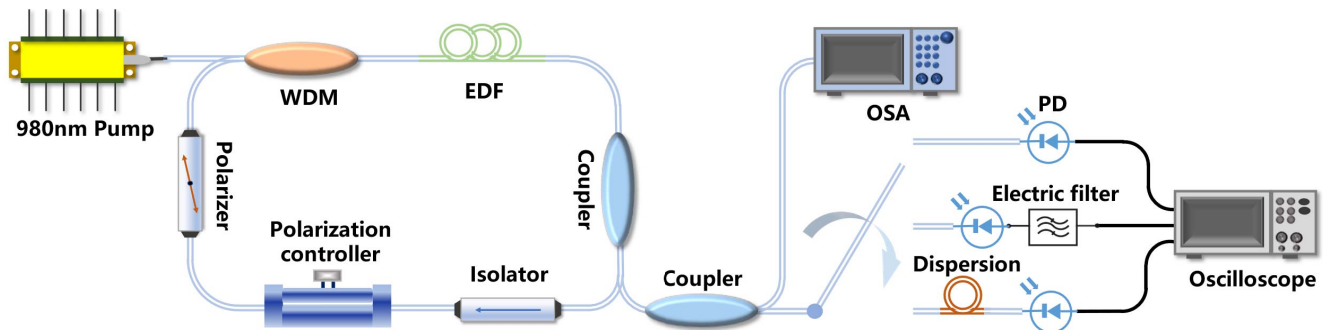


Fig. 1. The experimental setup to explore pulse broadening effects. WDM, wavelength division multiplexing; EDF, erbium-doped fibre; PD, photodiode; OSA, optical spectrum analyzer. Fibre links are represented by blue lines and electrical links by black lines.

to obtain more sampling points in the pulse region. There are two methods to broaden the pulses. One is the equivalent spectrum filtering effect realized by properly reducing the bandwidth of the acquisition system. The alternative is to impose a spectral phase to the optical pulse via a dispersion medium, which is termed as the pre-stretch technique. The two methods are experimentally compared and the pre-stretch technique manifests salient signal-to-noise ratio (SNR) thereby obtaining the much larger countable threshold range (CTR), a threshold selection range to achieve correct pulse counting in time domain. Later, the CTR will be elucidated in detail.

As illustrated in Fig. 1, a home-built erbium-doped MLFL is used to study the output pulse train with different detection methods. The laser consists of a 50-cm long erbium-doped fibre (EDF, Er-110dB/m), an isolator for unidirectional operation and a coupler for signal output. A 980 nm pump is served as the energy source to produce a C-band signal in the EDF through a wavelength division multiplex (WDM). A polarizer and a manual polarization controller (PC) are incorporated into the cavity for the NPE mode-locking. The total cavity length is 4.25 m corresponding to a fundamental repetition rate of 48 MHz.

The output pulse train is digitized by an oscilloscope where the sample rate is fixed at 500 MSa/s, to simulate the low-sampling-rate situation. For comparison, there are 3 methods to receive the optical pulse train. In the first method (i.e., the top branch in the right portion of Fig. 1), the optical signal is directly detected by a 10 GHz photodiode (PD). The second method (i.e., the middle branch in the right portion of Fig. 1) is to append a low-pass electrical filter between the PD and the oscilloscope. The last method (i.e., the bottom branch in the right portion of Fig. 1) is to pre-stretch the pulses through a dispersion medium, and then detected by the same PD. With a 3-dB optical coupler, half portion of the output power from the laser cavity is sent to an optical spectrum analyzer (OSA) for spectra monitoring and recording.

Electrical pulse trains obtained through 3 methods are shown in Fig. 2(a) with a time window of 0.4 μ s. The bandwidth of the low-pass filter is 200 MHz and the dispersion medium is a span of dispersion compensation fibre with a total dispersion of 170 ps/nm. It is obvious that several pulses are missing when using the direct detection method because of the limited sampling rate. The situation becomes better when using the low-pass filtering before the PD and there is no omitted pulse due to the temporal broadening effect brought by the

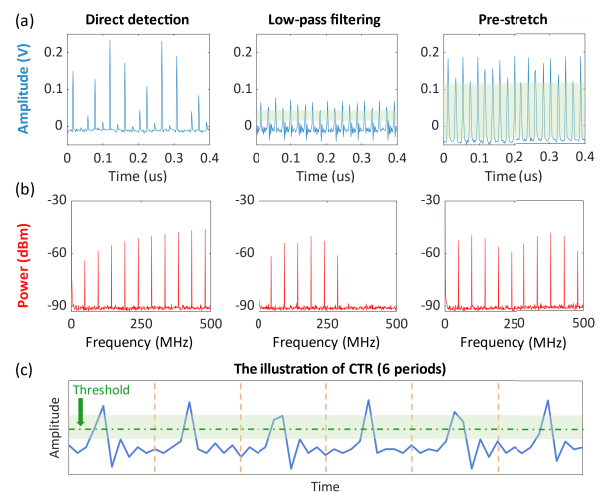


Fig. 2. Pulse broadening effect comparison and the illustration of the CTR. (a) The oscilloscope traces. (b) The electrical frequency spectra. From left to right: the methods of direct detection, with the low-pass filtering and with the pre-stretch technique. (c) The illustration of setting the threshold and CTR, where the green area indicates the CTR.

low-pass filtering. However, since the high-frequency energy is blocked, the overall energy and the SNR are very low after the low-pass filtering. The pulse train obtained by the pre-stretch technique also contains each pulse and has a much better SNR. The left inset in Fig. 2(b) shows the standard comb-like frequency spectrum of the mode-locked pulse train using the direct detection method, while the high-frequency components are removed in the low-pass filtering method as shown in the middle of Fig. 2(b). Compared to the frequency spectrum using direct detection, the frequency spectrum obtained by the pre-stretch method retains the substantial frequency domain characteristics. Moreover, the proportion of low-frequency components increase due to the stretching effect over pulses of the dispersion, thereby improving the sampling effect over short pulses under a low sampling rate.

The temporal pulse counting method is used for mode-locked states discrimination and a pre-set threshold is required for the pulse counting. In a single period, the pulse is counted after the sampled amplitude surpasses the threshold and then falls below the threshold. Therefore, there are two basic requirements for the discrimination of the fundamental mode-locking state, do not omit pulses and do not count multiple pulses in a single period. It is obvious that the threshold setting

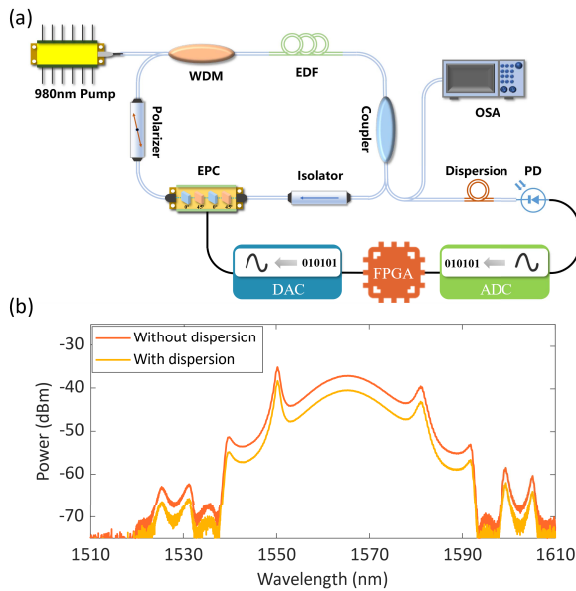


Fig. 3. (a) The experimental setup for the pre-stretch technique enabled 48 MHz AML. EPC, electronic polarization controller; ADC, analog-to-digital converter; DAC, digital-to-analog converter; FPGA, field-programmable gate array. Fibre links are represented by blue lines and electrical links by black lines. (b) The output optical spectra with (yellow) and without (orange) the dispersion.

is closely related to the discrimination result. However, the reasonable threshold is not sole.

For a temporal waveform of some mode-locking state, there is a CTR for threshold selection to obtain the correct pulse counting result. A larger CTR represents the stronger robustness against various disturbances and the smaller pulse counting errors. Fig. 2(c) shows an example of 6 periods and the CTR is highlighted in green. Likewise, the CTR is highlighted in green in Fig. 2(a). Apparently, the CTR of the pre-stretch method is way larger than that of the low-pass filtering method benefitted from the high SNR.

To validate the pre-stretch technique in high-repetition-rate AML, as shown in Fig. 3(a), we perform automatic mode-locking over a 48 MHz MLFL using the pre-stretch technique, where the sampling rate of the 8-bits ADC is 400 MSa/s and the dispersion amount is 170 ps/nm. Different from the typical NPE laser structure in Fig. 1, the manual PC is replaced with an electronic polarization controller (EPC), which consists of 4 phase-retard crystals oriented in different directions. The 4 phase-retard crystals inside the EPC are controlled by a 4-channel DC voltage signal thereby the intracavity polarization state can be altered. The automatic mode-locking depends on the real-time feedback hardware where an FPGA serves as the operation core. The dispersed pulse train is firstly converted to an electrical signal by the PD and then sampled by the ADC to FPGA for the pulse-counting-based mode-locking discrimination and optimization based on our previously proposed advanced Rosenbrock search (ARS) [17]. Then, according to the indication of the optimization algorithm, the EPC is controlled by 4 digital-to-analog converters (DACs). The orange curve in Fig. 3(b) shows the spectrum of the fundamental mode-locking state automatically searched by the ARS, which is a typical soliton spectrum

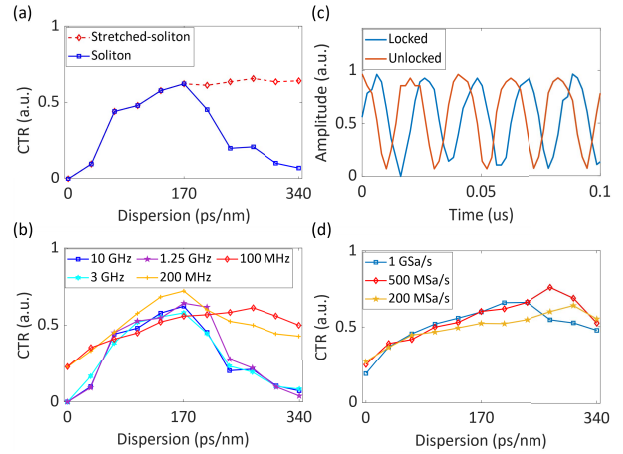


Fig. 4. (a) Under the fixed sampling rate of at 500 MSa/s and the fixed bandwidth of 10 GHz, the CTR varies with the dispersion amount for the pre-stretch in the soliton laser with negative net dispersion (blue line), and in the stretched-soliton laser with near-zero net dispersion (red line). (b) Under a fixed sampling rate of 500 MSa/s, to investigate the relation among the dispersion amount, the CTR, and different electrical bandwidths including 10 GHz (blue line), 3 GHz (light blue line), 1.25 GHz (purple line), 200 MHz (yellow line), and 100 MHz (red line). (c) Under a fixed sampling rate of 500 MSa/s and a fixed bandwidth of 50 MHz, the normalized waveform contrast between fundamental mode-locking state (blue line) and unlocked state (orange line). (d) Under a fixed bandwidth of 100 MHz, to investigate the relation among the dispersion amount, the CTR, and different sampling rates including 1 GSa/s, 500 MSa/s, and 200 MSa/s.

centred at 1565.3 nm with Kelly sidebands and has a spectral full width at half maximum (FWHM) of 14 nm. Note that the pump power is kept low in experiments to exclude the generation of bound states. To validate that the nonlinearities are negligible during pre-stretching, the spectrum after pre-stretch is measured as well and shown in the yellow curve in Fig. 3(b). Compared to the spectrum without pre-stretch, little change of the spectrum is observed except for the loss-induced power fading.

III. DISCUSSION

In order to explore the effect of dispersion amount on the CTR, we experimentally test different dispersion amount. The MLFL for the test runs in a net-negative dispersion regime, resulting in a soliton laser with Kelly sidebands on the spectrum. Note that the intensity of the temporal waveform is normalized, thus the CTR ranges from 0 to 1. The blue curve in Fig. 4(a) shows the calculated CTR obtained under different dispersion amount in experiments. In the dispersion amount ranging from 0 to 170 ps/nm, the CTR continues rising owing to the pre-stretch technique as expected. However, as the dispersion amount further increases, the stretched pulses start to overlap with each other and the Kelly sidebands emerge due to the time stretch effect [23], resulting in a rapid decline in the CTR. Therefore, in this case, the optimal dispersion amount is about 170 ps/nm with the largest CTR, which is inversely proportional to the spectral FWHM and the fundamental repetition rate.

Further, through ignoring the Kelly sidebands under the large dispersion amount, we predict the relation between the CTR and the dispersion amount in the stretched-soliton laser with near-zero net dispersion, as the red dashed curve in Fig. 4(a) shows. Different from the case in the soliton laser,

because there is no incorrect pulse counting induced by the Kelly sidebands, the CTR does not suffer a considerable drop after the dispersion amount exceeds 170 ps/nm. The CTR tends to converge due to the severe intra-pulse overlap and the lower SNR caused by the large dispersion.

The high-speed ADC considerably contributes to the overall cost. Therefore, the minimum required sampling rate and the bandwidth should be investigated when the pre-stretch technique is adopted. We firstly investigate the correlation between the bandwidth of the acquisition system and the dispersion amount. In the experiment, the PD has a 3-dB bandwidth of 10 GHz and the acquisition device is a 60-GHz Lecory real-time oscilloscope. Note that the acquisition bandwidth is the overall bandwidth of the PD and the acquisition system. Thus, the smaller acquisition bandwidth is modelled by adding a low-pass filter after the PD. As Fig. 4(c) shows, when the acquisition bandwidth is merely 50 MHz, it is impossible to discriminate the mode-locking states using the temporal waveform. Given such small acquisition bandwidth, the harmonic tones constitute the steep edges of the pulses are blocked. The remaining fundamental tone manifests itself as a sine wave in the time domain. Therefore, the minimum acquisition bandwidth for realizing automatic mode-locking is tested to be 100 MHz, which is about twice the fundamental repetition rate. Fig. 4(b) shows the relation between the acquisition bandwidth and the dispersion amount under a fixed sampling rate of 500 MSa/s. When the acquisition bandwidth is heavily reduced (i.e., 100 MHz in this case), the bandwidth limit induced pulse broadening becomes comparable to the dispersion induced pulse stretching, thereby shifting the optimal dispersion amount. Then, under the minimum acquisition bandwidth of 100 MHz, the relation between the sampling rate of the acquisition system and the dispersion amount is also investigated as shown in Fig. 4(d). The sampling rate ranges from 200 MSa/s to 1 GSa/s. The pulse-counting-based discrimination of mode-locking states expires when the sampling rate falls below 200 MSa/s and the situation resembles the case shown in Fig. 4(c). The minimum sampling rate is in accordance with the Nyquist's law.

IV. CONCLUSION

To summarize, we propose the dispersion-enabled pre-stretch technique as an effective method for reducing both the sampling rate and bandwidth of the acquisition system in the automatic mode-locking area. With the pre-stretch technique, a 48-MHz real-time AML is demonstrated, where the discrimination of mode-locking states is realized by an ADC with a sampling rate of merely 400 MSa/s. Further, the correlations among the dispersion amount of the pre-stretch, the bandwidth, and the sampling rate of the acquisition system are experimentally investigated. A preliminary conclusion can be drawn from the results. To apply the automatic mode-locking technique to a MLFL, the bandwidth of the acquisition system should be above twice of the fundamental repetition rate. Accordingly, the sampling rate of the acquisition system should be larger than twice of the minimum bandwidth, which is four times of the fundamental repetition rate. Besides, the empirical solution for the optimal dispersion amount of the pre-stretch is

illuminated, which is highly related to the spectral bandwidth and the fundamental repetition rate. We believe this work accelerates the emergence of the low-cost real-time AMLs with even higher repetition rates thereby breeding more high-frame-rate metrological applications based on femtosecond pulses.

REFERENCES

- [1] X.-Q. Liu *et al.*, "Biomimetic sapphire windows enabled by inside-out femtosecond laser deep-scribing," *PhotonIX*, vol. 3, no. 1, pp. 1–13, Dec. 2022.
- [2] K. Sugioka and Y. Cheng, "Ultrafast lasers—Reliable tools for advanced materials processing," *Light, Sci. Appl.*, vol. 3, no. 4, p. e149, Apr. 2014.
- [3] N. Picqué and T. W. Hänsch, "Frequency comb spectroscopy," *Nature Photon.*, vol. 13, no. 3, pp. 146–157, 2019.
- [4] M. J. Redlich *et al.*, "High-pulse-energy multiphoton imaging of neurons and oligodendrocytes in deep murine brain with a fiber laser," *Sci. Rep.*, vol. 11, no. 1, pp. 1–11, Dec. 2021.
- [5] C. Xu and F. W. Wise, "Recent advances in fibre lasers for nonlinear microscopy," *Nature Photon.*, vol. 7, pp. 875–882, Oct. 2013.
- [6] N. Nemitz *et al.*, "Frequency ratio of Yb and Sr clocks with 5×10^{-17} uncertainty at 150 seconds averaging time," *Nature Photon.*, vol. 10, no. 4, pp. 258–261, Apr. 2016.
- [7] B. J. Bloom *et al.*, "An optical lattice clock with accuracy and stability at the 10^{-18} level," *Nature*, vol. 506, no. 7486, pp. 71–75, Feb. 2014.
- [8] C.-H. Li *et al.*, "A laser frequency comb that enables radial velocity measurements with a precision of 1 cm s^{-1} ," *Nature*, vol. 452, no. 7187, pp. 610–612, Apr. 2008.
- [9] S. A. Diddams, K. Vahala, and T. Udem, "Optical frequency combs: Coherently uniting the electromagnetic spectrum," *Science*, vol. 369, no. 6501, Jul. 2020, Art. no. eaay3676.
- [10] T. Hellwig, T. Walbaum, P. Groß, and C. Fallnich, "Automated characterization and alignment of passively mode-locked fiber lasers based on nonlinear polarization rotation," *Appl. Phys. B, Lasers Opt.*, vol. 101, no. 3, pp. 565–570, 2010.
- [11] X. Shen, Q. Hao, and H. Zeng, "Self-tuning mode-locked fiber lasers based on prior collection of polarization settings," *IEEE Photon. Technol. Lett.*, vol. 29, no. 20, pp. 1719–1722, Oct. 15, 2017.
- [12] X. Wu, J. Peng, S. Boscolo, Y. Zhang, C. Finot, and H. Zeng, "Intelligent breathing soliton generation in ultrafast fiber lasers," *Laser Photon. Rev.*, vol. 16, no. 2, Feb. 2022, Art. no. 2100191.
- [13] X. Wei, J. C. Jing, Y. Shen, and L. V. Wang, "Harnessing a multi-dimensional fibre laser using genetic wavefront shaping," *Light, Sci. Appl.*, vol. 9, no. 1, pp. 1–10, Dec. 2020.
- [14] X. Fu, S. L. Brunton, and J. N. Kutz, "Classification of birefringence in mode-locked fiber lasers using machine learning and sparse representation," *Opt. Exp.*, vol. 22, no. 7, pp. 8585–8597, 2014.
- [15] T. Baumeister, S. L. Brunton, and J. N. Kutz, "Deep learning and model predictive control for self-tuning mode-locked lasers," *J. Opt. Soc. Amer. B, Opt. Phys.*, vol. 35, no. 3, pp. 617–626, 2018.
- [16] U. Andral *et al.*, "Toward an autotuning mode-locked fiber laser cavity," *J. Opt. Soc. Amer. B, Opt. Phys.*, vol. 33, no. 5, pp. 825–833, 2016.
- [17] G. Pu, L. Yi, L. Zhang, and W. Hu, "Intelligent programmable mode-locked fiber laser with a human-like algorithm," *Optica*, vol. 6, no. 3, pp. 362–369, 2019.
- [18] D. G. Winters, M. S. Kirchner, S. J. Backus, and H. C. Kapteyn, "Electronic initiation and optimization of nonlinear polarization evolution mode-locking in a fiber laser," *Opt. Exp.*, vol. 25, no. 26, pp. 33216–33225, 2017.
- [19] G. Pu, L. Yi, L. Zhang, C. Luo, Z. Li, and W. Hu, "Intelligent control of mode-locked femtosecond pulses by time-stretch-assisted real-time spectral analysis," *Light, Sci. Appl.*, vol. 9, no. 1, pp. 1–8, Dec. 2020.
- [20] R. I. Woodward and E. J. R. Kelleher, "Genetic algorithm-based control of birefringent filtering for self-tuning, self-pulsing fiber lasers," *Opt. Lett.*, vol. 42, no. 15, pp. 2952–2955, 2017.
- [21] H. Shi, Y. Song, F. Liang, L. Xu, M. Hu, and C. Wang, "Effect of timing jitter on time-of-flight distance measurements using dual femtosecond lasers," *Opt. Exp.*, vol. 23, no. 11, pp. 14057–14069, 2015.
- [22] I. Coddington, W. C. Swann, L. Nenadovic, and N. R. Newbury, "Rapid and precise absolute distance measurements at long range," *Nature Photon.*, vol. 3, pp. 351–356, May 2009.
- [23] A. Mahjoubfar, D. V. Churkin, S. Barland, N. Broderick, S. K. Turitsyn, and B. Jalali, "Time stretch and its applications," *Nature Photon.*, vol. 11, pp. 341–351, Jun. 2017.